Measurement of the vector character of electric fields by optical second-harmonic generation

J. I. Dadap, J. Shan, and A. S. Weling

Departments of Physics and Electrical Engineering, Columbia University, New York, New York 10027

J. A. Misewich

IBM T. J. Watson Research Center, P.O. Box 218, Yorktown Heights, New York 10598

A. Nahata

AlliedSignal, Inc., P.O. Box 1021, Morristown, New Jersey 07962

T. F. Heinz

Departments of Physics and Electrical Engineering, Columbia University, New York, New York 10027

Received April 20, 1999

We present a scheme for the determination of the vector nature of an electric field by optical second-harmonic generation. We demonstrate the technique by mapping the two-dimensional electric-field vector of a biased transmission line structure on silicon with a spatial resolution of ~10 μm. © 1999 Optical Society of America

OCIS codes: 190.0190, 190.4350.

The capability of measuring electric fields with ultrafast time resolution is of interest and importance for both fundamental and technological reasons. A promising new technique for probing transient electric fields is optical second-harmonic generation (SHG). SHG has been employed to detect electrical pulses[1] and microwave signals in transmission line structures[2] as well as freely propagating terahertz radiation.[3] This method, which utilizes the nonresonant material response of the sample, provides exceptional time resolution. For current experimental implementations with state-of-the-art mode-locked lasers, a response time of ~10 fs may be expected. The approach of field-induced SHG complements the powerful and well-established laser-based techniques of electro-optic and photoconductive sampling.[4] The attractiveness of the SHG scheme lies in its simplicity and flexibility: For centrosymmetric materials, SHG permits direct optical probing of the field that is present in the sample without the introduction of external crystals or special device structures.

The motivation for applying the SHG process to probe electric fields lies in symmetry considerations. As is well known, SHG from centrosymmetric media is forbidden in the dipole approximation. The presence of an electric field $\mathbf{E}^0$, however, lifts the inversion symmetry of the material and causes the efficiency of SHG to be strongly modified, as has been observed in a variety of materials and structures.[1–3,5–7] Although previous studies have illustrated the sensitivity and the time resolution of the method for probing the strength of the electric field, to our knowledge the potential for determination of the *vector* character of the electric field has not been examined. In this Letter we present a scheme for such vector electric-field measurements. We illustrate the method by mapping the spatial distribution of the in-plane electric field in a silicon sample. In related studies with SHG, spatial mapping of ferroelectric and magnetic domains has been demonstrated.[8]

The principle for extracting information on the vector components of the electric field $\mathbf{E}^0$ of interest can be seen by examination of the field-induced nonlinear polarization at the second-harmonic (SH) frequency:

$$P_i^{2\omega} = \sum_{jkl} \chi_{ijkl}^{(3)} E_j^{\omega} E_k^{\omega} E_l^{0} \,. \qquad (1)$$

Here $\mathbf{E}^\omega$ denotes the pump laser field at fundamental frequency ω and $\chi_{ijkl}^{(3)}$ is the third-order nonlinear susceptibility tensor that is responsible for the field-induced SHG process. With respect to optical measurements, we can describe this nonlinear material response in the presence of field $\mathbf{E}^0$ as an effective second-order nonlinear susceptibility of $\chi_{ijk}^{(2),\mathrm{eff}} \equiv \sum_l \chi_{ijkl}^{(3)} E_l^0$.

In terms of this formulation, the extraction of the field vector $\mathbf{E}^0$ is conceptually clear. One performs appropriate measurements of the SHG process to determine the relevant values of $\chi_{ijk}^{(2),\mathrm{eff}}$.[7] $\mathbf{E}^0$ can then be inferred from a comparison of $\chi_{ijk}^{(2),\mathrm{eff}}$ and the known (or separately measured) values of $\chi_{ijkl}^{(3)}$. Here we restrict our attention to materials of cubic or higher symmetry. In this case the form of $\chi_{ijkl}^{(3)}$ is considerably simplified, having as independent elements only $\chi_{iiii}^{(3)}$, $\chi_{iijj}^{(3)}$, $\chi_{ijij}^{(3)}$, and $\chi_{ijji}^{(3)}$, where $\{i, j\} = \{x, y, z\}$ and $i \neq j$ correspond to the crystalline axes. Two useful relations that follow for symmetry-allowed elements of $\chi_{ijk}^{(2),\mathrm{eff}}$ are

$$\chi_{iii}^{(2),\mathrm{eff}} = \chi_{iiii}^{(3)} E_i^0 \,, \qquad (2a)$$

$$\chi_{jii}^{(2),\mathrm{eff}} = \chi_{jiij}^{(3)} E_j^0 \,. \qquad (2b)$$

0146-9592/99/151059-03$15.00/0

Either of these equations alone is, in principle, sufficient for deducing all three components of $\mathbf{E}^0$. If we consider a pump laser field that is polarized along the y direction, Eqs. (2) yield

$$\chi_{xyy}^{(2),\mathrm{eff}} = \chi_{xyyx}^{(3)} E_x^0 , \tag{3a}$$

$$\chi_{yyy}^{(2),\mathrm{eff}} = \chi_{yyyy}^{(3)} E_y^0 , \tag{3b}$$

$$\chi_{zyy}^{(2),\mathrm{eff}} = \chi_{zyyz}^{(3)} E_z^0 . \tag{3c}$$

By measuring the SH signals for various polarization configurations and incidence angles, we can obtain the effective susceptibilities $\chi_{xyy}^{(2),\mathrm{eff}}$, $\chi_{yyy}^{(2),\mathrm{eff}}$, and $\chi_{zyy}^{(2),\mathrm{eff}}$, as is well established for surface SHG measurements.[7] From an appropriate set of calibration measurements, which yield the susceptibilities $\chi_{xyyx}^{(3)} = \chi_{zyyz}^{(3)}$, and $\chi_{yyyy}^{(3)}$, all three components of $\mathbf{E}^0$ can be deduced from Eqs. (3). Polarization-dependent measurements, it should be noted, have been employed for extracting the vector components of the field by electro-optic sampling in an external crystal.[9]

In the present investigation we restrict our considerations for reasons of simplicity to a determination of the in-plane components of the electric field in an isotropic material or (100) face of a cubic medium. In this instance one can identify a convenient experimental scheme by use of laser excitation at normal incidence. For this geometry, Eqs. (1), (3a), and (3b) yield the field-dependent SH radiation, $E_{\mathrm{FD},i}^{2\omega} \propto P_i^{2\omega}$, with components

$$E_{\mathrm{FD},x}^{2\omega} = f\chi_{xyyx}^{(3)} (E_y^{\omega})^2 E_x^0 , \tag{4a}$$

$$E_{\mathrm{FD},y}^{2\omega} = f\chi_{yyyy}^{(3)} (E_y^{\omega})^2 E_y^0 , \tag{4b}$$

where f is a proportionality constant that depends on the Fresnel factors at the input and output wavelengths. Equations (4) reveal a direct one-to-one mapping of the in-plane components, E_x^0 and E_y^0, of the applied electric field $\mathbf{E}^0$ onto the corresponding components of the radiated SH field. After an appropriate calibration E_x^0 and E_y^0 can thus be determined just by rotation of the analyzer to yield the desired projection of $\mathbf{E}^0$.

In SH measurements the intensity $I_{2\omega}$, which is proportional to $|\mathbf{E}^{2\omega}|^2$, is detected. In the absence of a field-independent background, as was the case for this study, information on the sign of the probed electric-field components is lost. Interference techniques are thus necessary to characterize fully the field.[10,11] Here we have applied a homodyne detection scheme that not only recovers the sign of the field but also linearizes the response of the measured SH to the electric-field strength.[11] Briefly, the SH field of interest, $E_{\mathrm{FD},i}^{2\omega}$, is combined with a strong reference SH field (local oscillator), $E_{\mathrm{ref},i}^{2\omega} \gg E_{\mathrm{FD},i}^{2\omega}$, so that the two fields are in phase. The measured SH intensity polarized along direction i then becomes

$$I_{2\omega,i} \propto |E_{\mathrm{ref},i}^{2\omega} + E_{\mathrm{FD},i}^{2\omega}|^2 \approx |E_{\mathrm{ref},i}^{2\omega}|^2 + 2E_{\mathrm{ref},i}^{2\omega} E_{\mathrm{FD},i}^{2\omega} . \tag{5}$$

Hence it follows from Eqs. (4) and (5) that $I_{2\omega,i} \propto E_i^0$.

Figure 1 illustrates the experimental setup schematically. The source of the SH probe radiation is a mode-locked Ti:sapphire laser, which produces pulses of 60-fs duration at a wavelength of 775 nm and a repetition rate of 80 MHz. The y-polarized laser beam is focused at normal incidence on the silicon sample with an average power of 180 mW. Before it reaches the sample, the fundamental beam is transmitted through a dichroic beam splitter. The beam also passes through a z-cut quartz crystal of 250-μm thickness, which generates the SH reference beam that is required for the homodyne detection scheme.[11] The SH radiation arising from both the sample and reference is reflected by the dichroic beam splitter and, after it passes through appropriate filters and a polarizer, is detected with gated photon-counting electronics. Both x and y polarizations of the SH radiation were detected.

Our sample was a silicon-on-sapphire substrate on which aluminum strip lines were deposited. The electrode geometry, shown in Fig. 1, consists of two 750 μm $\times$ 750 μm rectangular pads that are separated by 80 μm. Since the photon energy for the pump radiation in this measurement lay slightly above the bandgap, the absorption of pump radiation led to a certain degree of heating (<1 K) as well as to carrier generation in the sample. To reduce these effects one should choose a source of radiation with a photon energy lying below the bandgap. The sample was ion implanted, which rendered the 0.6-μm-thick silicon epilayer isotropic and the metallic contacts ohmic. Ion implantation also reduced the carrier lifetime significantly, thereby decreasing the screening of the bias field by the photogenerated carriers.[12] For purposes of illustration a bias voltage of 360 V, corresponding to an average electric-field strength of approximately 45 kV/cm, was applied across the electrodes. The resistance between the electrodes had an average value of 5 MΩ under laser irradiation, similar to the value without laser exposure, and no appreciable current-induced heating was observed. The sensitivity of this technique has been established to be $\sim$100 (V/cm)/Hz$^{1/2}$, which should be amenable to

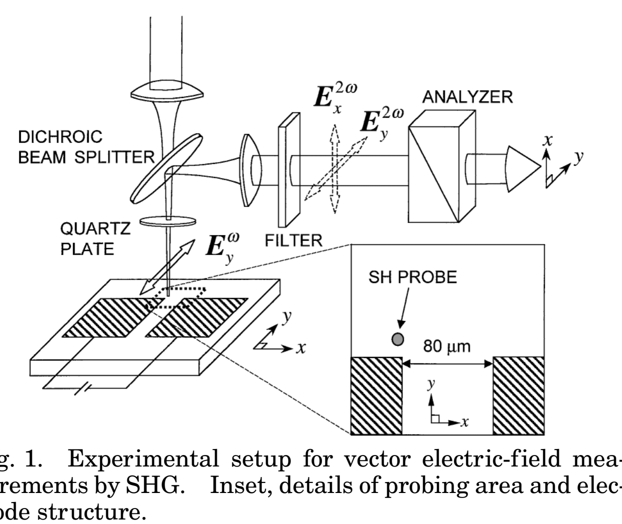

Fig. 1. Experimental setup for vector electric-field measurements by SHG. Inset, details of probing area and electrode structure.

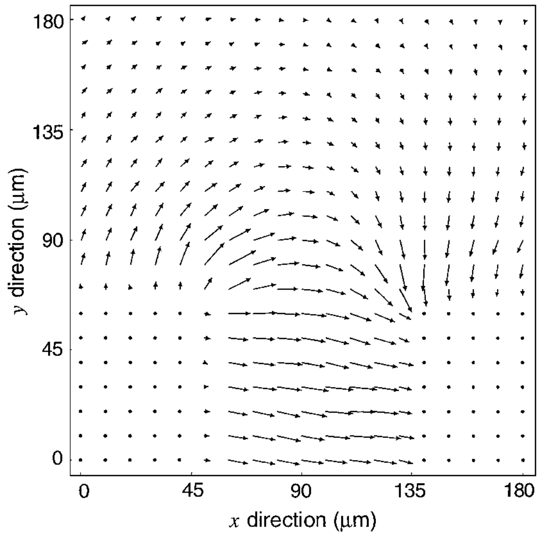

Fig. 2. Experimental results: vector map of the electric field $\mathbf{E}^0$.

further optimization through improvements in laser and material parameters.[11] We sampled the electric-field components by scanning along the x axis for each y position at 10-μm increments in a 180 μm $\times$ 180 μm square grid (inset of Fig. 1). For each sampling point the total data-collection time was 8 s, with a typical count rate of 10^5 Hz. The measurements were made differentially by subtraction of the signal in the absence of the electric field from that for an applied bias. The spatial resolution, which corresponds to a SH beam diameter of 14 μm at the sample, was determined by measurement of the change in the SH signal as the reference beam traveled across the boundary between the silicon and the metallic electrode.

Using the formalism discussed above, we obtained the in-plane components, E_x^0 and E_y^0, of the field $\mathbf{E}^0$ at each grid point. Figure 2 shows the resulting vector map of the electric field. Notice that in the area between the electrodes the electric field is aligned along the x direction, as expected. We attribute the weak irregularities in the electric-field direction that can be seen in certain spatial regions to local imperfections and inhomogeneities in the substrate and electrode structure. In the region beyond the end of the electrodes we observe the expected fringing pattern. The electric field in this region has both x and y components, which can be comparable, especially near the corners of the electrodes. Because of the finite spatial resolution of the SHG probe, the inferred amplitude of the electric field at grid points adjacent to the electrodes is reduced and, conversely, finite values for the electric field are found for grid points just inside the electrodes. Well inside the electrodes, no electric field was detected within experimental uncertainty.

A necessary step in this experiment is the calibration of the SH response for electric-field components along each of the x and y directions. For this purpose an applied field directed at an angle of 45° with respect to the polarization of the input laser beam was produced by rotation of the sample about its surface normal. Comparing the SH signals that were polarized along the original orthogonal axes of the analyzer, we then obtained the relative sensitivity of the measurement to the orthogonal components of $\mathbf{E}^0$. An absolute calibration of sensitivity can also be made in this fashion, assuming that the strength of the electric field for the calibration is already known.

To summarize, we have presented a general scheme for measuring the vector character of electric fields by use of SHG, and we have demonstrated the method by mapping the spatial distribution of the in-plane electric field in a silicon sample. We are exploring the application of this technique to the study of the dynamics of changing polarization states of high-frequency electric fields.

This work was funded by the U.S. Air Force Office of Scientific Research (grant F49620-98-1-0137), the National Science Foundation (grant CHE-96-12294), and the Joint Services Electronics Program (grant DAAG55-97-1-0166). T. F. Heinz's e-mail address is tony.heinz@columbia.edu.

References

1. A. Nahata, T. F. Heinz, and J. A. Misewich, Appl. Phys. Lett. **69,** 746 (1996).
2. C. Ohlhoff, C. Meyer, G. Lüpke, T. Löffler, T. Pfeifer, H. G. Roskos, and H. Kurz, Appl. Phys. Lett. **68,** 1 (1996).
3. A. Nahata and T. F. Heinz, Opt. Lett. **23,** 67 (1998).
4. D. H. Auston, in *Ultrashort Laser Pulses: Generation and Applications*, 2nd ed., W. Kaiser, ed. (Springer-Verlag, Berlin, 1993), pp. 183 and 445.
5. C. H. Lee, R. K. Chang, and N. Bloembergen, Phys. Rev. Lett. **18,** 167 (1967); O. A. Aktsipetrov, A. A. Fedyanin, V. N. Golovkina, and T. V. Murzina, Opt. Lett. **19,** 1450 (1994); J. I. Dadap, X. F. Hu, M. H. Anderson, M. C. Downer, J. K. Lowell, and O. A. Aktsipetrov, Phys. Rev. B **53,** R7607 (1996); J. Bloch, J. G. Mihaychuk, and H. M. van Driel, Phys. Rev. Lett. **77,** 920 (1996); P. Godefroy, W. de Jong, C. W. van Hasselt, M. A. C. Devillers, and Th. Rasing, Appl. Phys. Lett. **68,** 1982 (1996).
6. G. L. Richmond, J. M. Robinson, and V. L. Shannon, Prog. Surf. Sci. **28,** 1 (1988); R. M. Corn and D. A. Higgins, Chem. Rev. **94,** 107 (1994); K. B. Eisenthal, Chem. Rev. **96,** 1343 (1996).
7. T. F. Heinz, in *Nonlinear Surface Electromagnetic Phenomena*, H.-E. Ponath and G. I. Stegeman, eds. (North-Holland, Amsterdam, 1991), p. 353; G. A. Reider and T. F. Heinz, in *Photonic Probes of Surfaces*, P. Halevi, ed. (Elsevier, Amsterdam, 1995), p. 413.
8. Y. Uesu, S. Kurimura, and Y. Yamamoto, Appl. Phys. Lett. **66,** 2165 (1995); V. Kirilyuk, A. Kirilyuk, and Th. Rasing, Appl. Phys. Lett. **70,** 2306 (1997).
9. T. Itatani, T. Nakagawa, F. Kano, K. Ohta, and Y. Sugiyama, IEICE Trans. Electron. **E78-C,** 73 (1995).
10. R. Stolle, G. Marowsky, E. Schwarzberg, and G. Berkovic, Appl. Phys. B **63,** 491 (1996), and references therein; P. Wilson, Y. Jiang, O. A. Aktsipetrov, E. D. Mishina, and M. C. Downer, Opt. Lett. **24,** 496 (1999).
11. J. I. Dadap, J. Shan, A. S. Weling, J. A. Misewich, and T. F. Heinz, Appl. Phys. B **68,** 333 (1999).
12. J. I. Dadap, P. T. Wilson, M. H. Anderson, M. C. Downer, and M. ter Beek, Opt. Lett. **22,** 901 (1997).